

## Josephson oscillations in binary mixtures of $F=1$ spinor Bose-Einstein condensates

B. Juliá-Díaz,<sup>1</sup> M. Guilleumas,<sup>1</sup> M. Lewenstein,<sup>2,3</sup> A. Polls,<sup>1</sup> and A. Sanpera<sup>2,4</sup>

<sup>1</sup>*Departament d'Estructura i Constituents de la Matèria, Universitat de Barcelona, 08028 Barcelona, Spain*

<sup>2</sup>*Institució Catalana de Recerca i Estudis Avançats (ICREA), Lluís Companys 23, 08010 Barcelona, Spain*

<sup>3</sup>*Institut de Ciències Fotòniques (ICFO), Castelldefels, 08860 Barcelona, Spain*

<sup>4</sup>*Grup de Física Teòrica, Universitat Autònoma de Barcelona, 08193 Bellaterra, Spain*

(Received 25 February 2009; published 21 August 2009)

We analyze theoretically Josephson oscillations in a mixture of two Zeeman states of a spinor Bose-Einstein condensate in a double-well potential. We find that in the strongly polarized case, the less populated component exhibits a complex dynamics with an anti-Josephson behavior, i.e., oscillates in phase with the more populated one. In the balanced population case, the Josephson oscillations unveil a dependence with the different spin collision channels. This effect could be used to experimentally measure the distinct scattering lengths entering in the description of a spinor condensate. Our numerical results are in close agreement with an analytical description of the binary mixture using a two-mode model.

DOI: [10.1103/PhysRevA.80.023616](https://doi.org/10.1103/PhysRevA.80.023616)

PACS number(s): 03.75.Lm, 03.75.Kk, 03.75.Mn, 74.50.+r

Tunneling is one of the most fascinating quantum phenomena known since the development of quantum mechanics. At macroscopic scale, the Josephson effect essentially consists on the fast oscillating tunneling through a macroscopic barrier driven by a quantum phase difference between the two sides of the potential barrier [1].

Josephson dynamics of individual atoms has been theoretically studied by several groups [2]. Its extension to the tunneling of a Bose-Einstein condensate (BEC) in a two-well potential was presented in [3]. On the experimental side, Josephson tunneling of BEC in an optical lattice was first reported in Ref. [4]. Recently, a clear evidence of a bosonic Josephson junction in a weakly linked scalar BEC has been presented [5]. There, the observed time evolution of both the phase difference between the two sides of the barrier and the population imbalance shows the importance of the interactions and is accurately described by directly solving the full Gross-Pitaevskii (GP) equation or by using a two-mode approximation [6].

Multicomponent BECs trapped in double wells offer an interesting extension of the tunneling problem. Binary mixtures (i.e., pseudospin-1/2 BECs) that support density-density interactions have been analyzed in Refs. [7,8] using mainly the two-mode approach. More complex spinor BECs that support population transfer between different Zeeman states have been also studied as possible atomic candidates for the macroscopic quantum tunneling of magnetization (MQTM) [9,10].

In this work, we investigate the dynamics of a weakly linked mixture of  $m = \pm 1$  Zeeman components of a  $F=1$  spinor  $^{87}\text{Rb}$  condensate. By solving the GP equation, we find that in the strongly polarized case, the less-populated component oscillates in phase with the more populated one. For equal populations, the corresponding Josephson frequency provides information about the different scattering lengths of the system. We show how these two combined setups give access to the spin-dependent interaction strength. Our method extracts information from the macroscopic dynamics of the two Zeeman components on a two-well potential. It can be seen as the macroscopic counterpart of the method of

Ref. [11] where the spin dynamics of many atom pairs is considered based on an earlier observation of coherent spin dynamics of ultracold atom pairs trapped in sites of an optical lattice in a Mott insulator regime. Our method would improve the current knowledge which despite the accuracy of their involved experiments cannot, for instance, uniquely determine whether the  $F=2$  ground state of  $^{87}\text{Rb}$  is in an antiferromagnetic or a cyclic phase [11].

Following the conditions used in the experiments of Josephson tunneling in a scalar condensate [5], we consider  $N=1150$  atoms of spin-1  $^{87}\text{Rb}$  trapped initially in the following potential:

$$V(\mathbf{r}) = (M/2)(\omega_x^2 x^2 + \omega_y^2 y^2 + \omega_z^2 z^2) + V_0 \cos^2[\pi(x - \Delta_m)/q_0],$$

with  $\omega_x = 2\pi \times 78$  Hz,  $\omega_y = 2\pi \times 66$  Hz,  $\omega_z = 2\pi \times 90$  Hz,  $q_0 = 5.2 \mu\text{m}$ ,  $V_0 = 413h$  Hz, and  $M$  is the mass of the atom.  $\Delta_m$  defines the initial asymmetry in the double-well potential and thus is directly related to the initial population imbalance. At  $t=0$ , the small asymmetry is switched off ( $\Delta_m=0$ ) and the system is let to evolve in the double-well potential, which is the same for all components. The fact that the double well is created only along the  $x$  direction forces the dynamics of the Josephson oscillation to be one dimensional as beautifully demonstrated in [5]. Then, defining  $\omega_{\perp} = \sqrt{\omega_x \omega_y}$ , the coupling constants can be rescaled by a factor  $1/(2\pi a_{\perp}^2)$ , with  $a_{\perp}$  the transverse oscillator length and the dynamical equations transform into one-dimensional ones [12].

In the mean-field approach, the  $F=1$  spinor condensate is described by a vector order parameter  $\Psi$  whose components  $\psi_m = |\psi_m| e^{i\varphi_m}$  correspond to the wave function of each magnetic sublevel  $|F=1, m\rangle \equiv |m\rangle$ , with  $m=1, 0, -1$ . In absence of an external magnetic field and at zero temperature, the spin dynamics of this system confined in an external potential,  $V$ , is described by the following coupled equations for the spin components [13]:

$$i\hbar \frac{\partial \psi_{\pm 1}}{\partial t} = [\mathcal{H}_s + c_2(n_{\pm 1} + n_0 - n_{\mp 1})] \psi_{\pm 1} + c_2 \psi_0^2 \psi_{\mp 1}^*,$$

$$i\hbar \frac{\partial \psi_0}{\partial t} = [\mathcal{H}_s + c_2(n_1 + n_{-1})]\psi_0 + c_2 2\psi_1 \psi_0^* \psi_{-1}, \quad (1)$$

with  $\mathcal{H}_s = -\hbar^2/(2M)\nabla^2 + V + c_0 n$  being the spin-independent part of the Hamiltonian. The density of the  $m$ th component is given by  $n_m(\mathbf{r}) = |\psi_m(\mathbf{r})|^2$ , while  $n(\mathbf{r}) = \sum_m |\psi_m(\mathbf{r})|^2$  is the total density normalized to the total number of atoms  $N$ . The population of each hyperfine state is  $N_m = \int d\mathbf{r} |\psi_m(\mathbf{r})|^2$ . The couplings are  $c_0 = 4\pi\hbar^2(a_0 + 2a_2)/(3M)$  and  $c_2 = 4\pi\hbar^2(a_2 - a_0)/(3M)$ , where  $a_0$  and  $a_2$  are the scattering lengths describing binary elastic collisions in the channels of total spin 0 and 2, respectively. Their values are  $a_0 = 101.8a_B$  and  $a_2 = 100.4a_B$  [14]. The interatomic interactions permit the transfer of population between the different Zeeman components by processes that conserve the total spin,  $|0\rangle + |0\rangle \leftrightarrow |+1\rangle + |-1\rangle$ . Therefore, in a spinor condensate, the number of atoms in each component is not a conserved quantity. Due to the chosen conditions, notably the small total number of atoms and the fact that we will consider an initial zero population of  $m=0$  atoms, the population transfer effects between the different components is very small [12]. Therefore, in our calculation, the number of atoms in each Zeeman sublevel remains constant in time as in a real binary mixture, but the spinor character is preserved through the parameter  $c_2$  which is the spin-dependent collision term.

In the considered double-well potential, we can define the population imbalances between the two sides of the trap for each component as  $z_m(t) = [N_{m,L}(t) - N_{m,R}(t)]/N_m(t)$ , where  $N_{m,L(R)}(t)$  corresponds to the population on the left (right) side of the trap. The other relevant quantity is the phase difference between both sides of the trap defined as  $\hat{\varphi}_m(t) = \hat{\varphi}_{m,R}(t) - \hat{\varphi}_{m,L}(t)$  for each component. The GP equation predicts the evolution of  $\varphi_m$  as a function of both  $t$  and  $x$ . Within our parameters, the condensates at each side of the trap remain mostly in a coherent state meaning that the  $x$  dependence of  $\varphi_m$  is fairly small, as shown in Fig. 1, where the condensates in each potential well have an almost constant phase. Thus, for simplicity, we define  $\hat{\varphi}_{m,L(R)}$  as the phase of  $\psi_m(x_M)$ , where  $x_M$  is the position of the maximum density of each condensate.

For the sake of clarity, we start by analyzing as a reference the scalar Josephson effect. To this aim, we put all the atoms in a single component and solve the corresponding time-dependent GP equation equivalent to the scalar case with a nonlinear term proportional to  $c_0 + c_2$ . In Fig. 1, we show the time evolution of the population imbalance and phase difference for  $\Delta = -0.20 \mu\text{m}$ . Both quantities oscillate with a frequency  $\omega_J$  which slightly differs from the bare Rabi frequency (noninteracting limit) by a term proportional to the interactions [3]. Two snapshots of the density profile at  $t=0$  and  $t=10$  ms can be seen in the inset.

New interesting phenomena appear when a binary mixture is considered. The binary mixture is simulated by means of Eqs. (1) with an initial zero amount of  $m=0$  atoms. We have checked, however, that all the results presented in this paper are nevertheless stable against the presence of a small amount of  $m=0$  atoms in the trap ( $N_0/N \leq 1\%$ ). We consider  $\Delta_{\pm 1} = \mp 0.10 \mu\text{m}$ , which produces asymmetric initial den-

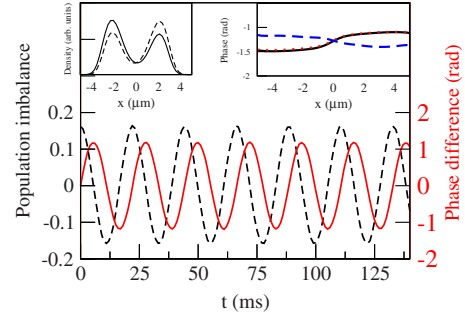


FIG. 1. (Color online) Time evolution of the population imbalance (dashed) and phase difference (solid) for a scalar BEC. The upper left inset depicts a snapshot of the population density at  $t=0$  ms (solid) and  $t=10$  ms (dashed). The upper right inset shows the phase as a function of  $x$  at  $t=120$  ms. Solid line stands for the scalar BEC with initial population imbalance 0.06. Dashed and dotted lines correspond, respectively, to the  $m=+1$  and  $m=-1$  components of a simulation with  $(N_1/N, N_0/N, N_{-1}/N) = (5\%, 0\%, 95\%)$  and  $z_{\pm 1}(0) = \mp 0.06$ . In all cases, the initial phase is set to zero for all  $x$ .

sity profiles for both components with imbalances of  $z_{\pm 1}(0) = \mp 0.06$ . The configurations considered are  $N_{-1}/N = 95\%$  and  $N_1/N = 5\%$  and no initial phase difference.

The system evolves in the following way. The most populated component essentially drives the dynamics; its population imbalance and phase difference (see Fig. 2) follow a behavior qualitatively and quantitatively similar to that of the scalar condensate. Whereas the less populated component,  $m=+1$  in this case, follows the dynamics of the other one. First, it does an “anti-Josephson” tunneling, i.e., the absolute value of its population imbalance actually grows driven by the other component, contrary to what would have happened in the absence of the other component. This is essentially due to the prevalence of the interaction with the other component over the population-imbalance-driven Josephson tunneling. In addition to the high-frequency Josephson oscillation,  $\omega_J$ , the less populated component has an additional lower fre-

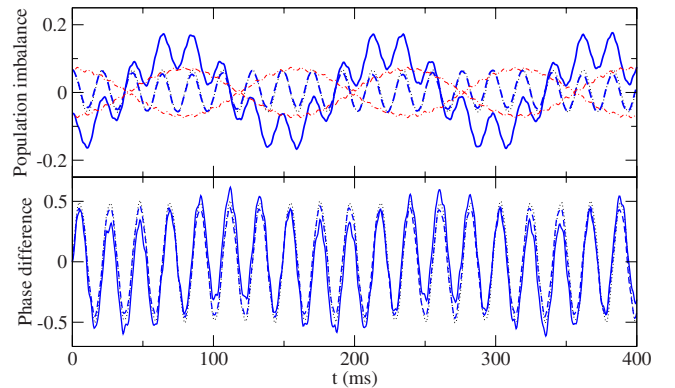


FIG. 2. (Color online) Population imbalance (upper panel) and phase difference (lower panel) between the two sides of each condensate. Dotted (black) line corresponds to the scalar case, solid and dashed blue lines correspond to the  $m=+1$  and  $m=-1$  components of a simulation with  $(5\%, 0\%, 95\%)$ . Red dot-dashed lines correspond to the  $(50\%, 0\%, 50\%)$  case.

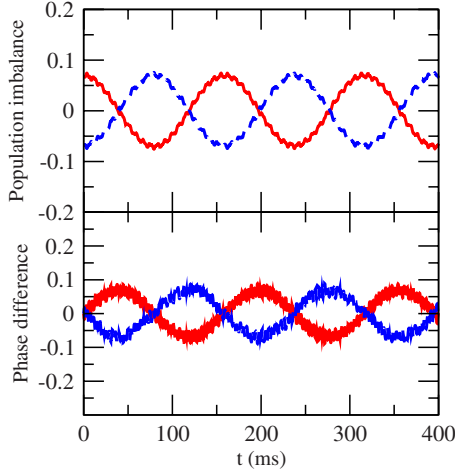


FIG. 3. (Color online) Population imbalance (upper panel) and phase difference (lower panel) between the two sides of each BEC for a simulation with (50%, 0%, 50%). Solid (red) lines correspond to the  $m=-1$  atoms and dashed (blue) lines to the  $m=+1$  atoms.

quency oscillation with a period of nearly 150 ms. Both effects will be analyzed below within the two-mode approximation.

A second interesting configuration is that of having the same population for both  $m=\pm 1$  components (50%, 0%, 50%) with the same initial population imbalance as before,  $z_{\pm 1}(0) = \mp 0.06$ . In this case, the behavior is completely different. Essentially, as can be seen in Fig. 3, a Josephson tunneling with an oscillation period of approximately 150 ms (almost 6 times larger than in the scalar case) is observed for both components. Thus, the longer oscillation, which actually corresponds to the lower frequency oscillation seen in Fig. 2, is a pure effect of having a binary mixture.

To get a deeper insight on the observed behavior, we have performed a two-mode analysis of a binary mixture of BECs. The general coupled GP equations for a binary mixture of components  $a$  and  $b$ , which keeps invariant the total number of atoms of each species, can be written as

$$i\hbar \frac{\partial \Psi_a}{\partial t} = \left[ -\frac{\hbar^2 \nabla^2}{2m_a} + V_a + g_{aa} |\Psi_a|^2 + g_{ab} |\Psi_b|^2 \right] \Psi_a,$$

$$i\hbar \frac{\partial \Psi_b}{\partial t} = \left[ -\frac{\hbar^2 \nabla^2}{2m_b} + V_b + g_{bb} |\Psi_b|^2 + g_{ba} |\Psi_a|^2 \right] \Psi_b. \quad (2)$$

These general couplings,  $g_{ij}$ , can be related to the  $c_0$  and  $c_2$  ones entering in Eqs. (1) as  $g_{aa} = g_{bb} = c_0 + c_2$  and  $g_{ab} = g_{ba} = c_0 - c_2$ . Since for  $^{87}\text{Rb}$  atoms in  $F=1$ ,  $|c_2| \ll c_0$ , the mixture we are considering has the same self-interaction between each component and similar to the mixing term,  $g_{ab} \sim g_{aa}$ .

The two-mode approximation can be expressed with the following ansatz [3]:  $\Psi_j = \Psi_{jL}(t)\Phi_{jL}(r) + \Psi_{jR}(t)\Phi_{jR}(r)$ , with  $\langle \Phi_{i\alpha} | \Phi_{j\beta} \rangle = \delta_{ij} \delta_{\alpha\beta}$  and  $\Psi_{j,\alpha}(t) = \sqrt{N_{j,\alpha}(t)} e^{i\phi_{j,\alpha}(t)}$ ,  $i, j = a, b$ , and  $\alpha, \beta = L, R$ . Equations for the coefficients  $\Psi_{i,\alpha}(t)$  are obtained from Eqs. (2), neglecting terms involving mixed products of  $L$  and  $R$  wave functions of order larger than 1. Rewritten in terms of the imbalances  $z_j(t) = [N_{jL}(t) - N_{jR}(t)] / N_j(t)$  and

phase differences  $\phi_j = \phi_{jR} - \phi_{jL}$ , they take the form

$$\dot{z}_a = -\omega_r \sqrt{1 - z_a^2} \sin \phi_a, \quad \dot{z}_b = -\omega_r \sqrt{1 - z_b^2} \sin \phi_b,$$

$$\dot{\phi}_a = \frac{U}{\hbar} N_a z_a + \frac{\tilde{U}}{\hbar} N_b z_b + \frac{\omega_r z_a}{\sqrt{1 - z_a^2}} \cos \phi_a,$$

$$\dot{\phi}_b = \frac{U}{\hbar} N_b z_b + \frac{\tilde{U}}{\hbar} N_a z_a + \frac{\omega_r z_b}{\sqrt{1 - z_b^2}} \cos \phi_b, \quad (3)$$

where  $\omega_r = 2K/\hbar$  denotes the Rabi frequency and

$$K = - \int d\mathbf{r} \left[ \frac{\hbar^2}{2M} \nabla \Phi_L(\mathbf{r}) \cdot \nabla \Phi_R(\mathbf{r}) + \Phi_L(\mathbf{r}) V \Phi_R(\mathbf{r}) \right],$$

$$U_{ij} = g_{ij} \int d\mathbf{r} \Phi_{i,L}^2(\mathbf{r}) \Phi_{j,L}^2(\mathbf{r}) = g_{ij} \int d\mathbf{r} \Phi_{i,R}^2(\mathbf{r}) \Phi_{j,R}^2(\mathbf{r}).$$

In Eqs. (3), we have considered a symmetric double well and the same mass for the particles of both components  $m_a = m_b \equiv M$ , thus defining  $\Phi_{L(R)} \equiv \Phi_{a,L(R)} = \Phi_{b,L(R)}$ . This yields  $U_{aa} = U_{bb} \equiv U$  and  $U_{ab} = U_{ba} \equiv \tilde{U}$ . The stability of these equations has been analyzed in Ref. [8].

The dynamics obtained by solving the coupled GP Eqs. (1) can be now understood by taking the appropriate limits on Eqs. (3) after linearizing them around the equilibrium values  $z_a = z_b = 0 = \phi_a = \phi_b$ . Defining  $\alpha$  and  $\beta$  as  $N_a = N(1 - \alpha)$ ,  $N_b = N\alpha$ , and  $\tilde{U} = U(1 + \beta)$ , Eqs. (3) reduce to

$$\dot{z}_a = -\omega_r \phi_a, \quad \dot{z}_b = -\omega_r \phi_b,$$

$$\dot{\phi}_a = [(1 - \alpha)NU/\hbar + \omega_r] z_a + \alpha(1 + \beta)NU/\hbar z_b,$$

$$\dot{\phi}_b = (1 - \alpha)(1 + \beta)NU/\hbar z_a + [\alpha NU/\hbar + \omega_r] z_b. \quad (4)$$

These equations correspond to two coupled nonrigid pendulums with normal-mode frequencies  $\omega_>$  and  $\omega_<$ . In our system,  $g_{ab} \sim g_{aa} = g_{bb}$ , i.e.,  $\tilde{U} \sim U$  and thus  $\beta \ll 1$ . Then, the eigenfrequencies can be approximated by  $\omega_> = \omega_r + (NU/\hbar)\alpha\beta(\alpha - 1)$ ,  $\omega_< = \omega_r [1 + NU/\hbar \omega_r (1 + \alpha\beta - \alpha^2\beta)] / \sqrt{1 + NU/\hbar \omega_r}$ . The behavior observed in Fig. 2 is explained by taking  $\alpha \rightarrow 0$ . In this limit, the frequencies simplify to  $\omega_> = \omega_r$  and  $\omega_< = \omega_r \sqrt{1 + UN/(\hbar \omega_r)} = \omega_j$ . The highest populated component,  $z_a$ , decouples from the less populated and thus performs a Josephson oscillation, as shown in Fig. 2, with the same frequency as the scalar case  $\omega_j$ , and the less populated component oscillates with the two eigenfrequencies  $\omega_> = \omega_r$  and  $\omega_< = \omega_j$ .

The case of equal populations can also be addressed within Eqs. (4) by setting  $\alpha = 1/2$ . In this case, the long mode can be enhanced by starting with opposite initial imbalances as in Fig. 3. Then, both components oscillate with  $\omega_> = \omega_r - \frac{NU}{4\hbar} \beta \equiv \tilde{\omega}$ . Since  $\beta \ll 1$ , this explains the similarity between the oscillation frequency of the (50%, 0%, 50%) case studied and the long oscillation of the less populated component of the (50%, 0%, 95%) case (see Fig. 2). Let us

emphasize that the frequency shift with respect to the Rabi frequency,  $NU/(4\hbar)\beta$ , is a direct consequence of the difference between  $g_{aa}$  and  $g_{ab}$ , which in turn depend on the interaction strengths,  $c_0$  and  $c_2$ . Alternatively, if the scattering lengths are known, the Josephson oscillation provides a tool to determine with high precision the number of atoms.

It is important to mention that we have assumed zero temperature and therefore, no phase fluctuations are present in our calculation. Indeed, phase fluctuations will evidently destroy the phase coherence of the condensate in each potential well, leading to a complete suppression of Josephson oscillations. For very elongated systems, it is known that even at small temperatures, the phase of the condensate fluctuates [15]. However, in the setup we have considered, which is closely related to the experimental setup demonstrating Josephson oscillations in a scalar BEC [5], phase fluctuations due to thermal effects will remain small since the condensate is essentially three dimensional although the dynamics is one dimensional. A detailed analysis of possible noise sources using a two-mode approximation has been developed for a scalar condensate in a double-well potential in [6], showing that coherence is preserved at the temperatures at which the experiment runs and demonstrating also how coherence is lost by increasing the temperature. A similar analysis applies here with a spinor BEC.

Summarizing, we have addressed the problem of a binary mixture of BECs which is realized with a  $F=1$  spinor BEC

where the  $m=0$  component is not populated. The behavior of the mixture has been analyzed in two significant limits: a binary mixture with a large difference in the concentration of the two components and a binary mixture with equal amount of both components. Both cases have been studied with the GP equations and have also been scrutinized by employing a simple two-mode approximation.

An independent measurement of the Rabi frequency could be obtained from the long oscillation of the less populated component of Fig. 2. That would allow for precise determination of the (otherwise difficult to measure, cf. [11]) spin-dependent interaction strength,  $a_2 - a_0$ , using the relations,  $(a_2 - a_0)/(a_0 + 2a_2) = -\beta/(2 + \beta)$  and  $\beta$  can be evaluated by using the above frequencies as  $\beta = 4\omega_r(\omega_r - \tilde{\omega})/(\omega_j^2 - \omega_r^2)$ . The accuracy of the method is expected to be comparable to that of Ref. [11] and is only constrained by the ability to measure with precision the different macroscopic oscillations. The method presented could be extended to any atom species and would be easy to generalize to the  $F=2$  case.

*Note added.* Recently, a related study appeared, reporting a two-mode study of binary mixtures [16].

We thank M. Oberthaler for encouraging us to develop this research direction. B.J.-D. is supported by a CPAN CSD Contract No. 2007-0042. This work is also supported by Grants No. FIS2008-01661, No. FIS2008-00421, No. FIS2008-00784, FerMix, and QOIT from MEC.

- 
- [1] A. J. Leggett *et al.*, *Rev. Mod. Phys.* **59**, 1 (1987).  
 [2] Q. Niu, X.-G. Zhao, G. A. Georgakis, and M. G. Raizen, *Phys. Rev. Lett.* **76**, 4504 (1996); S. R. Wilkinson, C. F. Bharucha, K. W. Madison, Q. Niu, and M. G. Raizen, *ibid.* **76**, 4512 (1996); M. Ben Dahan *et al.*, *ibid.* **76**, 4508 (1996); D. L. Haycock *et al.*, *ibid.* **85**, 3365 (2000).  
 [3] A. Smerzi, S. Fantoni, S. Giovanazzi, and S. R. Shenoy, *Phys. Rev. Lett.* **79**, 4950 (1997).  
 [4] C. Orzel *et al.*, *Science* **291**, 2386 (2001).  
 [5] M. Albiez, R. Gati, J. Fölling, S. Hunsmann, M. Cristiani, and M. K. Oberthaler, *Phys. Rev. Lett.* **95**, 010402 (2005).  
 [6] R. Gati and M. K. Oberthaler, *J. Phys. B* **40**, R61 (2007); D. Ananikian and T. Bergeman, *Phys. Rev. A* **73**, 013604 (2006).  
 [7] S. Ashhab and C. Lobo, *Phys. Rev. A* **66**, 013609 (2002); H. T. Ng, C. K. Law, and P. T. Leung, *ibid.* **68**, 013604 (2003); L. Wen and J. Li, *Phys. Lett. A* **369**, 307 (2007).  
 [8] X.-Q. Xu, L.-H. Lu, and Y.-Q. Li, *Phys. Rev. A* **78**, 043609 (2008).  
 [9] H. Pu, W. P. Zhang, and P. Meystre, *Phys. Rev. Lett.* **89**, 090401 (2002); Ö. E. Müstecaplıoğlu, W. Zhang, and L. You, *Phys. Rev. A* **75**, 023605 (2007).  
 [10] E. M. Chudnovsky and J. Tejada, *Macroscopic Quantum Tunneling of the Magnetic Moment*, Cambridge Studies in Magnetism (Cambridge University Press, Cambridge, England, 1998), Vol. 4.  
 [11] A. Widera *et al.*, *New J. Phys.* **8**, 152 (2006).  
 [12] M. Moreno-Cardoner, J. Mur-Petit, M. Guilleumas, A. Polls, A. Sanpera, and M. Lewenstein, *Phys. Rev. Lett.* **99**, 020404 (2007).  
 [13] T.-L. Ho, *Phys. Rev. Lett.* **81**, 742 (1998); T. Ohmi and K. Machida, *J. Phys. Soc. Jpn.* **67**, 1822 (1998).  
 [14] E. G. M. van Kempen, S. J. J. M. F. Kokkelmans, D. J. Heinzen, and B. J. Verhaar, *Phys. Rev. Lett.* **88**, 093201 (2002).  
 [15] D. S. Petrov, G. V. Shlyapnikov, and J. T. M. Walraven, *Phys. Rev. Lett.* **85**, 3745 (2000).  
 [16] I. I. Satija, R. Balakrishnan, P. Naudus, J. Heward, M. Edwards, and C. W. Clark, *Phys. Rev. A* **79**, 033616 (2009).